Hindawi
Advances in Civil Engineering
Volume 2022, Article ID 6045514, 16 pages
https://doi.org/10.1155/2022/6045514

Research Article

Static and Dynamic Compression Performances of Hybrid Fiber-Reinforced Lightweight Aggregate Concrete

Yan Zhou and Ming-Gao Chen

School of Architectural Engineering, Ma'anshan University, Ma'anshan 243000, China

Correspondence should be addressed to Yan Zhou; zhouy_2035@163.com

Received 4 October 2022; Revised 7 November 2022; Accepted 11 November 2022; Published 3 December 2022

Academic Editor: Piotr Smarzewski

In this study, basalt fiber and polypropylene fiber with different volume ratios were mixed into lightweight aggregate concrete (LAC), and the static compressive strength and dynamic compressive performance of LAC mixed with fiber were tested. The influence of basalt fiber and polypropylene fiber on the stress-strain relationship and energy conversion relationship of LAC was analyzed. The results show that basalt fiber and polypropylene fiber with an appropriate volume ratio are beneficial to enhance the strength and toughness of LAC, but the mixing effect is better. When the volume ratio of mixed fibers is 0.2%, the compressive strength, elastic modulus, peak strain, and ultimate strain are increased by 61.9%, 23.57%, 32.81%, and 45.14%, respectively, compared with the LAC without fibers. Based on the statistical damage theory, the compressive damage constitutive model of fiber LAC is established; fiber improves the ductility and energy absorption capacity of LAC and shows better impact resistance. Finally, based on modern SEM microscopic testing technology and EDS testing technology, the internal structure and chemical element composition of ordinary LAC and fiber lightweight aggregate were compared and analyzed. The internal compactness of the aggregate concrete improves the strength and toughness of the lightweight aggregate concrete, which reveals the mechanism of the fiber on the LAC from a microscopic point of view.

1. Introduction

At present, with the development of modern buildings towards large span and super high-rise buildings, to reduce structural section, reduce the weight of the structure, and improve the thermal insulation and other performances, the requirements of lightweight, high strength, durability, and sustainable development are put forward for concrete. Lightweight aggregate concrete (LAC) is widely used because of these advantages. LAC refers to the concrete that uses light aggregates to partially or completely replace coarse and fine aggregates and has the characteristics of high durability, fluidity, energy saving, and environmental protection, and the apparent density is not more than 1950 kg/m^3. Lightweight concrete and sublightweight concrete refer to the concrete in which part or all of the coarse aggregates are lightweight aggregates, and all-lightweight concrete refers to the concrete in which all the coarse and fine aggregates are made of lightweight aggregates [1–3]. At present, LAC is generally prepared from shale ceramsite, expansive clay ceramsite, or sintered ceramsite. Therefore, the promotion of lightweight aggregate concrete can make full use of various industrial and agricultural wastes, cut down on the amount of natural sand and stone, save energy, and reduce environmental pollution [4, 5]. The experimental study [4, 6] found that the mechanical strength and deformation ability of LAC were related to the type of lightweight aggregate, the water-binder ratio of the mixture, and the density grade. Compared to concrete with the same mix, the elastic modulus and stiffness of ordinary aggregate are larger than those of cement mortar, and the cracks generally expand from the interface area, while the elastic modulus and stiffness of lightweight aggregate are smaller than those of cement mortar. When subjected to external load, the cracks may pass through the lightweight aggregate itself, which makes the internal stress transfer mechanism different. The

tensile-compression strength ratio, flexural strength, elastic modulus and relative fracture energy of LAC are lower, and the peak compressive strain and brittleness are larger, with the increase of strength, the brittleness has a significant increase trend. Therefore, the strengthening and toughening of LAC have become a research hotspot in recent years.

At present, whether it is ordinary aggregate concrete or LAC, adding fiber is one of the methods recognized internationally that can massively reduce the brittleness of cement matrix materials and improve their strength and toughness [7–9]. For example, steel fiber, basalt fiber, glass fiber, polypropylene fiber, and carbon fiber. Previous studies [10–14] reported the compressive strength, toughness, impact resistance, and shear performance of steel fibers mixed with light aggregate concrete. Previous studies [15–22] reported the effect of carbon fiber on the strength, toughness, and thermal conductivity of lightweight aggregate concrete. Previous studies [22–26] reported analyzed the strength, impact, and shear properties of glass fiber LAC. But because of the high price of steel fiber and poor dispersion in the cement matrix, the complex manufacturing process of carbon fiber, and the alkali resistance of glass fiber in the cement matrix, problems such as sexuality restrict the application in practical engineering. Polypropylene fiber is a flexible fiber with high deformation performance, but its elastic modulus and tensile strength are relatively low. When incorporated into concrete, polypropylene fiber can reduce the expansion rate of macrocracks in concrete while improving concrete ductility [27–29]. Previous studies [30–35] reported the properties of polypropylene fiber reinforced LAC; the influence of compressive strength and elastic modulus is not obvious, but it can significantly increase the strength of LAC and can significantly enhance the toughness of LAC. Basalt fiber is made of basalt stone by high temperature and melting drawing, which is composed of SiO_2, Al_2O_3, CaO, MgO, Fe_2O_3, and TiO_2. On the one hand, the energy consumption in the preparation process of basalt fiber is low, and the elastic modulus can reach 93~115 GPa and the tensile strength can reach 200~5000 MPa, which is a new type of inorganic environmental protection, green, and high performance fiber material. On the other hand, basalt fiber has good bonding performance with cement-based materials [36–38]. The effect of basalt fiber on the strength, effect resistance, and shear performance of lightweight aggregate concrete was studied in references [39–41]. It is found that basalt fiber has great influence on compressive strength, impact resistance, and shear performance of lightweight aggregate concrete.

Studies have shown that [42–44] two or more fibers of different sizes are added to the concrete, which can reduce the generation of cracks in the concrete and have a positive effect on improving the toughness of the concrete. Therefore, when two kinds of fibers with different elastic moduli (basalt fiber and polypropylene fiber) are added to the LAC, the two can play the role of crack bridging at different structural scales, effectively inhibit the crack propagation of LAC, and improve the strength and toughness of LAC. At present, the research on mixed fiber lightweight aggregate concrete mainly focuses on the static strength and working performance, and there are few studies on the energy change law and dynamic compression performance during the static compression failure process. Based on this, to effectively promote the application of basalt-polypropylene hybrid fiber lightweight aggregate concrete in engineering structures, it is necessary to study the static compressive strength and dynamic compressive properties of LAC mixed with basalt fiber and polypropylene fiber. The influence of basalt fiber and polypropylene fiber on energy storage and dissipation during compression and impact failure of LAC was discussed from the perspective of energy conversion, and the compression constitutive model of basalt-polypropylene hybrid fiber lightweight aggregate concrete (HFLAC) was established according to the statistical damage theory. In order to provide a theoretical reference for the stress of high-rise or super high-rise lightweight aggregate concrete.

2. Trial Overview

2.1. Raw Materials. The cementitious material uses Chinese standard P O 42.5 grade ordinary Portland cement, and the 28-day compressive strength is 42.5 MPa. The coarse aggregate is shale ceramsite, and the fine aggregate is natural medium sand. The basic properties are shown in Table 1. To mix high elastic modulus and low elastic modulus fibers, the basalt fiber adopts chopped basalt fiber, and the polypropylene fiber adopts monofilament bundle polypropylene fiber. The basic properties are shown in Table 2. The water-reducing agent adopts HPWR-type high-performance water-reducing agents, and the water reduction rate is 37%. The water is ordinary tap water.

2.2. Mix Ratio Design. According to the preparation technology of lightweight aggregate concrete, the design coordination ratio is shown in Table 3.

2.3. Specimen Preparation. The production process of the specimen was as follows: the ceramsite and sand were mixed for 1 min, added with cement for 1 min, and then added with fiber for 2 min. After mixing evenly, the water-soluble water reducer was added for 3 min, and then the mixture was put into the mold to vibrate with a shaking table. Three 150 mm × 150 mm × 150 mm cube specimens were made in each group for the compressive strength test. HYE-3000 electro-hydraulic servo press was used for measurement, and the loading rate was 0.5 mm/s. Dynamic compression tests were performed using an aluminum split Hopkinson pressure bar (SHPB) device. The size of the specimen is 74 mm in diameter and 38 mm in height. Standard maintenance lasts 28 d. The test results were averaged.

3. Results and Discussion

3.1. Static Compressive Strength Test

3.1.1. Mechanical Properties Indicators

Table 1: Basic properties of aggregates.

Aggregate type	Aggregate particle size (mm)	Apparent density (kg/m^3)	Bulk density (kg/m^3)	Water absorption (%)	Cylinder strength (MPa)
Shale ceramsite	5~16	1512	860	2.2	6.9
Natural medium sand	4	2620	1510	1.9	—

Table 2: Fiber performance index.

Fiber type	Density (kg/m^3)	Length (mm)	Diameter (μm)	Elongation at break (%)	Elastic modulus (GPa)	Tensile strength (MPa)
Basalt fiber	2800	12	12	3.1	100	>4000
Polypropylene fiber	910	10	8	15	5.85	>700

Table 3: Mix proportion of HFLAC.

Specimen number	Material dosage (kg/m^3)						
	Cement	Sand	Ceramsite	Water	Water reducer	Basalt fiber	Polypropylene fiber
OC	450	1230	620	152	5.1	—	—
BC-0.1	450	1230	620	152	5.1	2.8	—
PC-0.1	450	1230	620	152	5.1	—	0.91
HC-0.1	450	1230	620	152	5.1	1.4	0.455
HC-0.2	450	1230	620	152	5.1	2.8	0.91
HC-0.3	450	1230	620	152	5.1	4.2	1.365
HC-0.4	450	1230	620	152	5.1	5.6	1.82

(1) Strength. The compressive strength values of each group of specimens are shown in Figure 1. It can be seen that the compressive strength of LAC shows a trend of increasing first and then decreasing. Compared with the LAC, the compressive strength increased by 61.9% when the fiber volume ratio was 0.2%.

(2) Elastic Modulus. The elastic modulus values of each group of specimens are shown in Figure 2. It can be seen from Figure 2 that the elastic modulus value gradually increases, but when the volume fraction exceeds 0.2%, the elastic modulus begins to decrease. When the fiber is mixed with fiber, the elastic modulus is larger than that of the single fiber. When the fiber volume ratio is 0.2, the elastic modulus value is the largest, which increases by 23.57% compared with the light aggregate concrete without fiber. The elastic modulus of LAC is clearly correlated with the elastic modulus of aggregate and surface structure. Fiber incorporation enhances the internal bonding of the specimen, so it can enhance the elastic modulus of LAC.

(3) Peak Strain. Peak strain is an important index in the stress-strain relationship of LAC, which is mainly affected by index such as strength, loading rate, pressure area, and constraint conditions. The peak strain of LAC is shown in Figure 3. It can be seen that with the upgrade of the fiber volume ratio, the peak strain of LAC increases gradually. When the volume ratio of mixed fibers is 0.2%, the peak strain increases by 32.81% compared with that of ordinary concrete without fibers. It shows that with the upgrade of fiber volume fraction, the deformation capacity of LAC increases, and the volume deformation rate increases gradually.

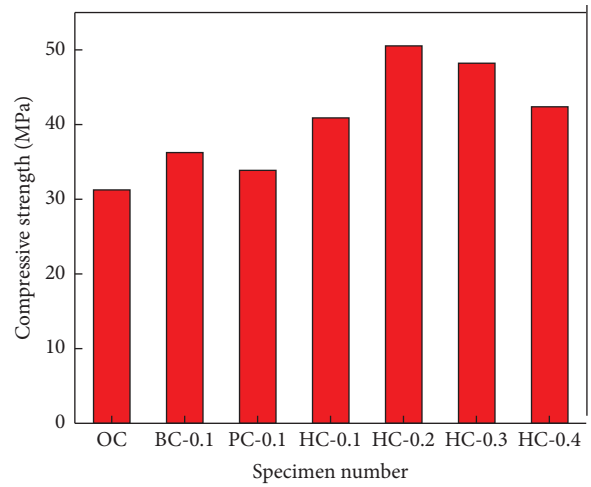

Figure 1: Compressive strength.

(4) Ultimate Strain. In the descending stage of the stress-strain curve, when the stress value is 75% of the peak stress value, the corresponding strain value at this time is called the ultimate strain. The ultimate strain is the stress-strain curve and its important characteristic points, which have important reference values for engineering applications. The ultimate strain of LAC is shown in Figure 4. It can be seen that the fiber increases the ultimate strain of the lightweight

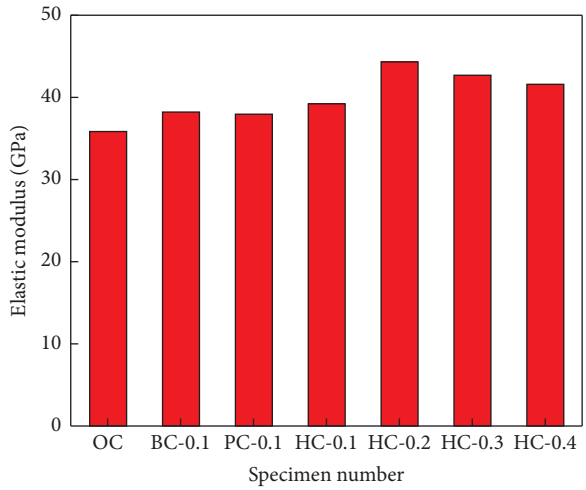

Figure 2: Elastic modulus.

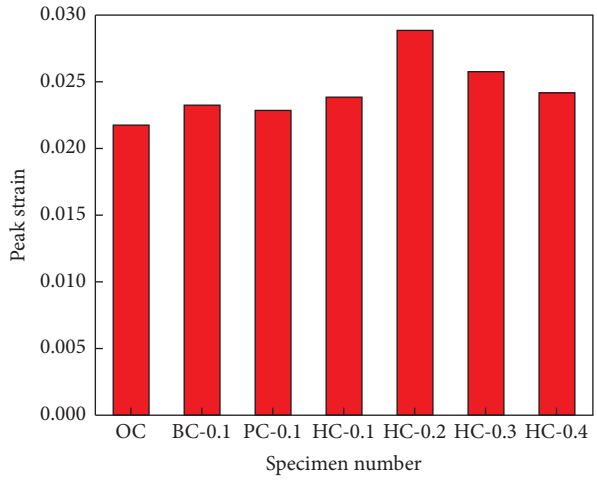

Figure 3: Peak strain.

aggregate concrete to a certain extent, which indicates that the ductility of the LAC can be effectively increased with the fiber. Among them, the ultimate strain value of the HC-0.2 group is the largest, which is 45.14% higher than that of the LAC without fibers.

3.1.2. Stress-Strain Relationship. The stress-strain curve can effectively reflect the damage change trend of concrete material under external load [45]. The full stress-strain curve of LAC is shown in Figure 5. It can be seen that there are four main stages before the peak of the compressive stress-strain curve of LAC appears. In the first stage, although there are pores and internal microcracks between the lightweight aggregate concrete matrix at the initial loading, the microcracks will not propagate due to the low load. In the second stage, the light aggregate concrete matrix begins to have local cracks, and the stress-strain curve begins to deviate from the linearity. In the third stage, at the interface between the cement matrix and the aggregate, the propagation of microcracks begins to appear unstable, and the

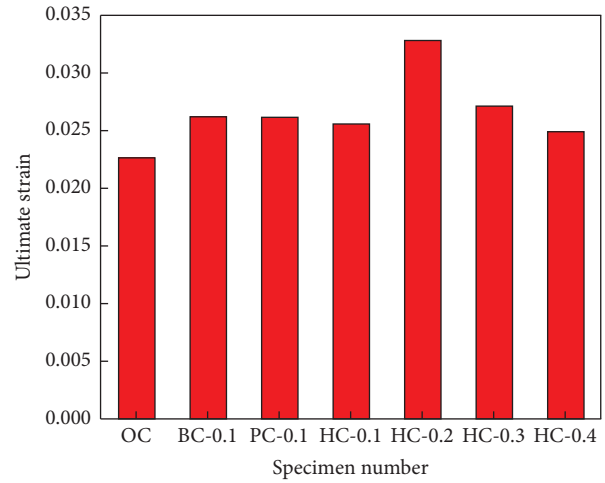

Figure 4: Ultimate strain.

cracks spread into the lightweight aggregate concrete in different paths. In the fourth stage, the main cracks grow steadily until one of the cracks reaches its critical width, at which point the specimen exhibits its peak stress.

It can be seen from Figure 5 that, in general, ordinary lightweight aggregate concrete exhibits obvious brittle failure, and the addition of fibers into the concrete makes the stress-strain curve more plump, showing a "high fat" shape. When the fiber volume fraction is 0.1%, compared with ordinary lightweight aggregate, although there is little difference before the peak stress, it significantly delays the decline rate of the stress-strain curve after the peak stress, indicating that fiber can obviously enhance the ductility deformation characteristics of lightweight aggregate concrete. By comparing the stress-strain curves of the BF-0.1 group and the PF-0.1 group, it can be seen that the influence of basalt fiber on the strength of LAC is greater than that of polypropylene fiber alone. However, after the peak stress, the decrease rate of the stress-strain curve of the BF-0.1 group is slightly larger than that of the PF-0.1 group, indicating that the ductility deformation of the LAC with polypropylene fiber alone is slightly larger than that with basalt fiber alone. When the volume fraction of hybrid fiber is 0.2%, the slope of the linear elastic stage of the stress-strain curve decreases, while the ductility deformation of lightweight aggregate concrete increases significantly. However, when the volume ratio of hybrid fiber is more than 0.2%, the dispersion uniformity of fiber in the LAC foundation is reduced, and it is prone to agglomerate. In the process of specimen production, bubbles are easily introduced, resulting in the increase of internal defects in lightweight aggregate concrete and the decrease of deformation resistance.

3.1.3. Energy Evolution Law. Energy evolution is the essential characteristic of concrete materials in the process of uniaxial compression failure [46]. In uniaxial compression, the essence of deformation and failure of concrete materials under load is the process of energy evolution inside concrete and energy exchange with the outside world [47]. The

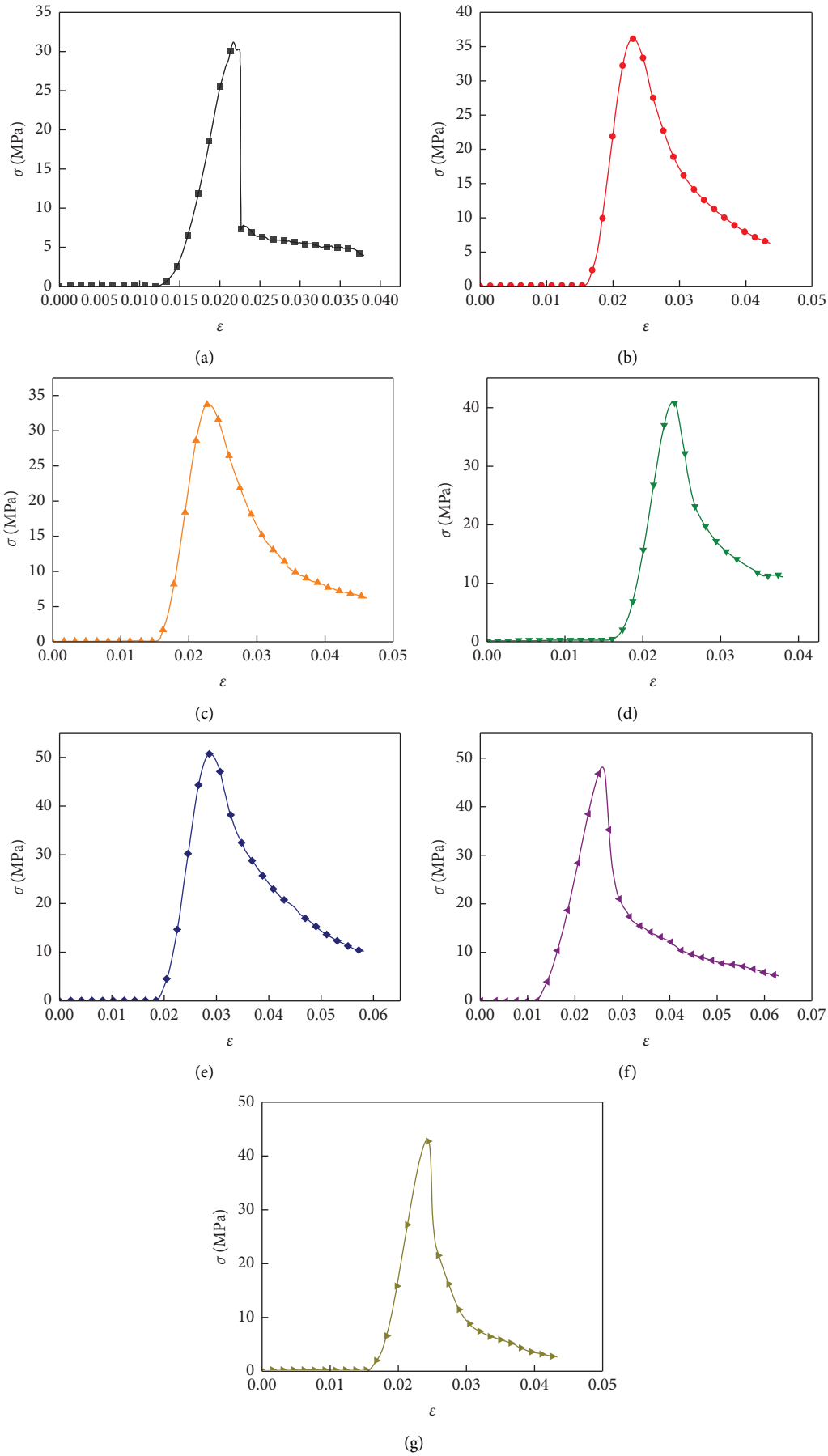

Figure 5: Stress-strain curve. (a) OC group. (b) BF-0.1 group. (c) PF-0.1 group. (d) HC-0.1 group. (e) HC-0.2 group. (f) HC-0.3 group. (g) HC-0.4 group.

evolution laws of total strain energy, dissipation energy, and elastic strain energy of LAC are shown in Figures 6–8, respectively. It can be seen that the energy evolution law can be divided into four stages: (1) Primary crack closure stage: the primary cracks in the lightweight aggregate concrete are closed under the initial load, and no new cracks are generated in the lightweight aggregate concrete at this time. The total strain energy and dissipated energy are small. (2) Linear elastic stage: at this time, no new cracks are formed in the lightweight aggregate concrete, the dissipation energy is still small, and at this time, the total strain energy is almost equal to the elastic strain energy. (3) Rapid expansion stage of cracks: at this time, new cracks begin to form inside the lightweight aggregate concrete, the total strain energy begins to gradually transform into dissipative energy, and the rate of increase of elastic strain energy decreases. (4) Crack penetration stage: after the peak stress, the cracks inside the lightweight aggregate concrete gradually penetrate, forming macroscopic penetration cracks. At this time, due to the gradual decrease of the load, the rate of increase of the total strain energy decreases, and the energy stored in the lightweight aggregate concrete is reduced. The elastic strain energy is dissipated in the form of dissipation energy due to the penetration of the crack. The elastic strain energy gradually decreases, and the dissipation energy increases rapidly.

Combining Figures 6–8 it can be seen that, when the fiber volume ratio is 0.1%, the influence of fibers on the energy evolution of LAC is small in the initial loading stage. With the increased load, the fiber can obviously improve the rate of increase of the total strain energy and dissipated energy of the LAC. When basalt fiber is mixed with polypropylene fiber, the total strain energy and dissipation energy of lightweight aggregate concrete increase significantly. Before the peak elastic strain energy, the influence of fiber type and volume rate on the variation law of concrete elastic strain energy is similar to the effect on the total strain energy and dissipated energy. After the peak elastic strain energy, the elastic strain energy of the OC group decreases rapidly, which indicates that the crack penetration speed is faster, showing obvious brittle failure characteristics. With the incorporation of fibers, especially the incorporation of hybrid fibers, the reduction rate of elastic strain energy gradually decreases, and the ductile failure characteristics increase. This is mainly because the bridging effect of basalt fiber and polypropylene fiber inhibits the rate of occurrence and development of cracks and significantly enhances the ductile failure characteristics of lightweight aggregate concrete.

3.1.4. Damage Constitutive Model. In 1986, the equivalent strain principle was proposed by Professor Lemaitre of France: under uniaxial loading, as long as the nominal stress in the constitutive relationship of non-destructive materials is changed by the valid stress after damage, the arbitrary strain constitutive relationship of damaged materials can be derived from the constitutive equation of non-destructive materials [48]. Based on this, the constitutive equation of

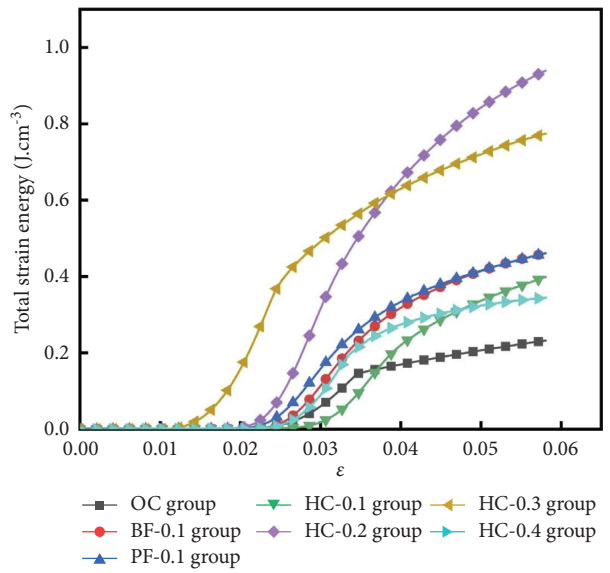

Figure 6: Evolution law of total strain energy.

damaged materials can be derived, as shown in the following equation:

$$\left.\begin{aligned} \varepsilon &= \frac{\sigma_n}{E} \\ \sigma_n &= \frac{\sigma}{1-D} \\ \varepsilon &= \frac{\sigma_n}{E} = \frac{\sigma}{E(1-D)} \end{aligned}\right\} \Rightarrow \sigma = E(1-D)E. \tag{1}$$

In equation (1), ε is the strain; σ_n is the valid stress; E is the elastic modulus of nondestructive material; D is the nominal stress; and D is the damage variable.

Assuming that the concrete damage parameter D obeys the Weibull statistical distribution, the damage constitutive model is deduced as follows:

$$\left.\begin{aligned} D &= 1 - \exp\left[-(\varepsilon/a)^b\right] \\ \sigma &= E(1-D)E \end{aligned}\right\} \Rightarrow \sigma = E\varepsilon \exp\left[-(\varepsilon/a)^b\right]. \tag{2}$$

In formula (2): a is the scale parameter; b is the shape parameter.

According to the characteristics of the stress-strain full curve, formula (2) should satisfy the following four conditions: ① $\sigma = 0, \varepsilon = 0$; ② $\varepsilon = 0, E = d\sigma/d\varepsilon$; ③ $\varepsilon = \varepsilon_c, \sigma = \sigma_c$; and ④ $\varepsilon = \varepsilon_c, d\sigma/d\varepsilon = 0$. Where ε_c is the peak strain; σ_c is the peak stress; and E is the initial elastic modulus. The following equation is derived

$$\frac{d\sigma}{d\varepsilon} = E \exp\left[(\varepsilon/a)^b\right]\left[1 - b(\varepsilon/a)^b\right]. \tag{3}$$

On substituting condition ④ into formula (3) we get the following equation:

$$\frac{d\sigma}{d\varepsilon} = E \exp\left[(\varepsilon_c/a)^b\right]\left[1 - b(\varepsilon_c/a)^b\right] = 0. \tag{4}$$

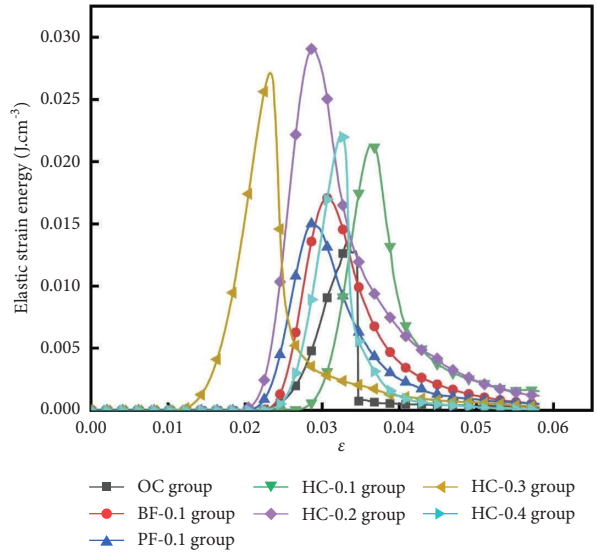

Figure 7: Evolution law of dissipative energy.

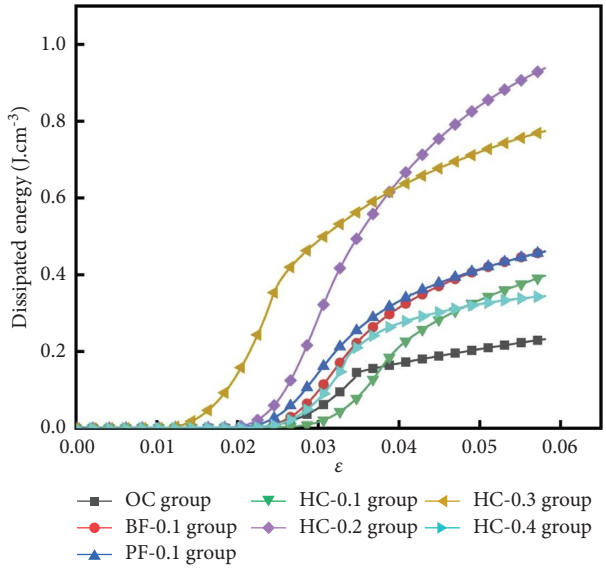

Figure 8: Evolution law of elastic strain energy.

Therefore,
$1 - b(\varepsilon_c/a)^b = 0 \Rightarrow b(\varepsilon_c/a)^b = 1 \Rightarrow a = \varepsilon_c/(1/b)^{1/b}$.

On substituting the condition ③ to get the following equation:

$$b = \frac{1}{\ln(E\varepsilon_c/\sigma_c)}. \tag{5}$$

The damage constitutive equation can be obtained as follows:

$$\sigma = E\varepsilon \exp\left[-(\varepsilon/a)^b\right]. \tag{6}$$

The damage evolution equation is as follows:

$$D = 1 - \exp\left[-(\varepsilon/a)^b\right]. \tag{7}$$

According to the measured peak stress, peak strain and initial elastic modulus, the damage constitutive equation and damage evolution equation of LAC under compression are shown in Table 4. Figure 9 is the comparison between the measured stress-strain curves and the theoretical curves obtained by using Table 4 constitutive equation. Figure 10 shows the damage evolution law of each group of specimens under compression.

As can be seen from Figure 9, on the whole, the constitutive model established based on damage theory can effectively represent the stress-strain relationship of LAC. Especially before the peak stress, it almost coincides, and the calculation results begin to deviate from the test results in the residual deformation stage. From Figure 10, it can be seen from the damage evolution law of LAC that before the peak

Table 4: Damage constitutive equation and damage evolution equation of LAC.

Specimen	Damage constitutive equation	Damage evolution equation
OC	$\sigma = 35877\varepsilon \exp\left[-(\varepsilon/0.00505)\right]^{0.31072}$	$D = 1 - \exp\left[-(\varepsilon/0.00505)\right]^{0.31072}$
BC-0.1	$\sigma = 38245\varepsilon \exp\left[-(\varepsilon/0.00561)\right]^{0.31246}$	$D = 1 - \exp\left[-(\varepsilon/0.00561)\right]^{0.31246}$
PC-0.1	$\sigma = 37967\varepsilon \exp\left[-(\varepsilon/0.00501)\right]^{0.30811}$	$D = 1 - \exp\left[-(\varepsilon/0.00501)\right]^{0.30811}$
HC-0.1	$\sigma = 39208\varepsilon \exp\left[-(\varepsilon/0.00672)\right]^{0.31962}$	$D = 1 - \exp\left[-(\varepsilon/0.00672)\right]^{0.31962}$
HC-0.2	$\sigma = 44333\varepsilon \exp\left[-(\varepsilon/0.00651)\right]^{0.30939}$	$D = 1 - \exp\left[-(\varepsilon/0.00651)\right]^{0.30939}$
HC-0.3	$\sigma = 42766\varepsilon \exp\left[-(\varepsilon/0.00725)\right]^{0.31957}$	$D = 1 - \exp\left[-(\varepsilon/0.00725)\right]^{0.31957}$
HC-0.4	$\sigma = 41954\varepsilon \exp\left[-(\varepsilon/0.00629)\right]^{0.31591}$	$D = 1 - \exp\left[-(\varepsilon/0.00629)\right]^{0.31591}$

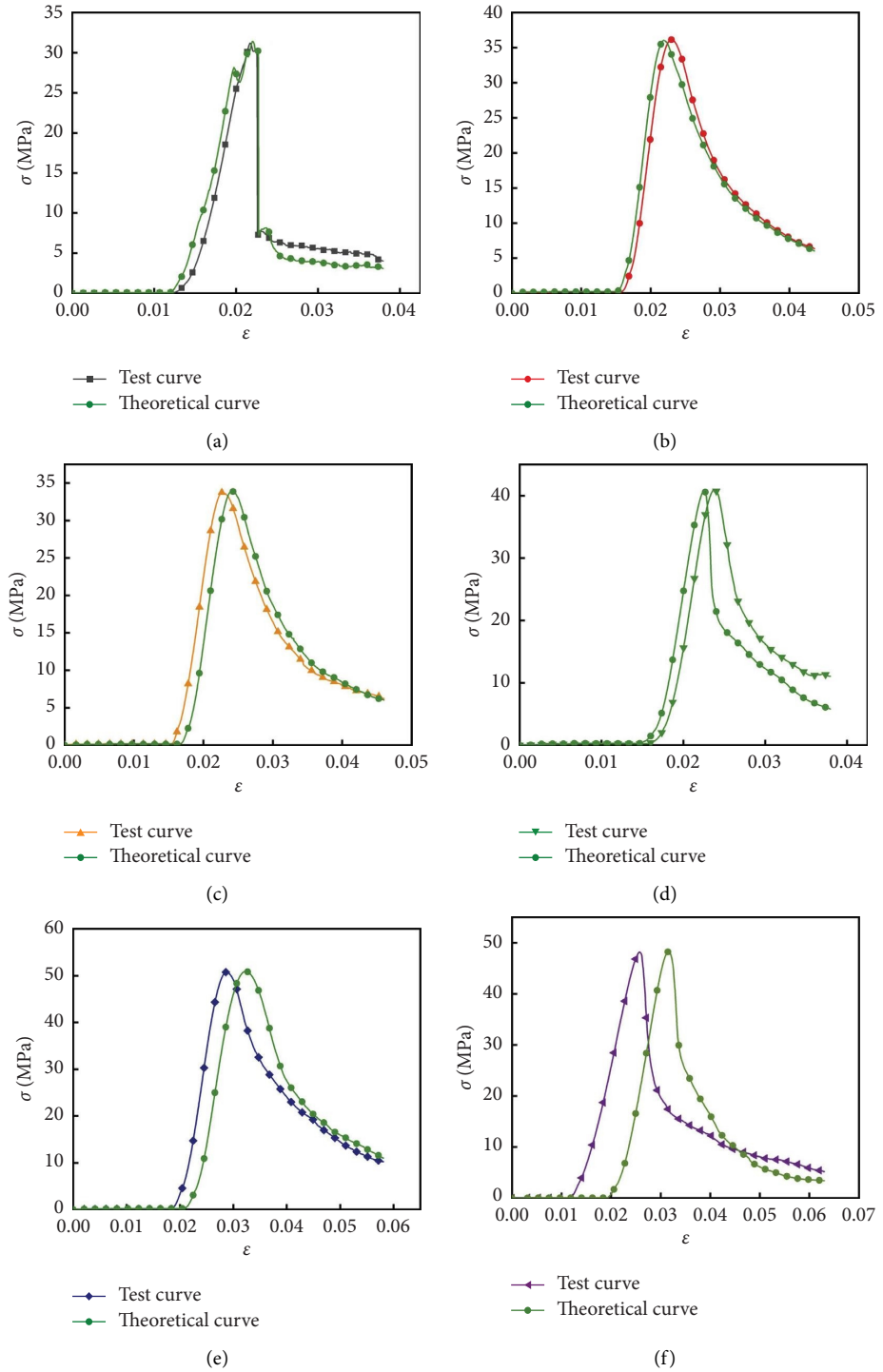

Figure 9: Continued.

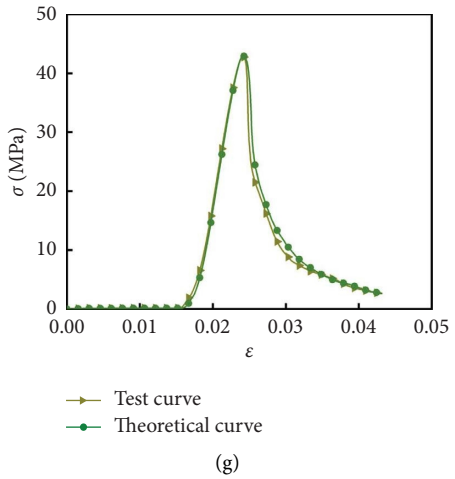

Figure 9: Comparison curve of LAC. (a) OC group. (b) BF-0.1 group. (c) PF-0.1 group. (d) HC-0.1 group. (e) HC-0.2 group. (f) HC-0.3 group. (g) HC-0.4 group.

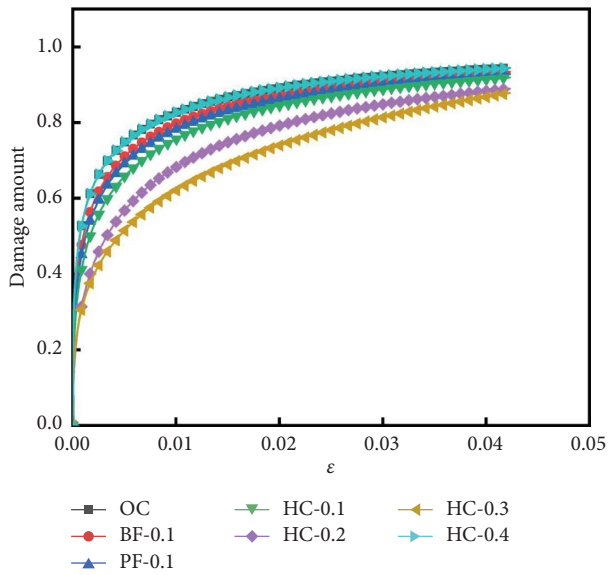

Figure 10: Damage evolution law.

stress, the damage of each group of specimens develops faster, but because the fibers can act as reinforcement, it can effectively reduce the weight of the lightweight aggregate concrete. The damage in the process of compressive deformation, after the peak stress, is also due to the bridging influence which effectively inhibits the expansion and penetration of cracks, reduces the damage development rate of LAC, and enhances the ductile deformation characteristics of LAC.

3.2. Dynamic Compression Performance Test

3.2.1. Stress-Strain Relationship. The stress-strain relationship of each group of specimens at 0.3 MPa air pressure is shown in Figure 11. It can be seen that the fiber type and content have a big effect on the stress-strain relationship of lightweight aggregate concrete. In the initial stage, the stress increases linearly with the increase in the strain. After reaching the elastic limit stress, the specimen enters a significant plastic shape in the deformation stage, accompanied by a slow increase in yield strength; when the yield stress is reached, the strain of the specimen upgrades slightly, but the stress decreases sharply, and the specimen is completely destroyed.

3.2.2. Mechanical Properties Parameters. Figure 12 shows the peak stress of LAC under the dynamic compression test. Figure 13 shows the peak strain of LAC under the dynamic compression test. The area enclosed by the curve and the coordinate axis represents the toughness index of the specimen under impact load. The toughness index of LAC is shown in Figure 14. The dynamic enhancement factor DIF is the ratio of the dynamic peak stress to the corresponding

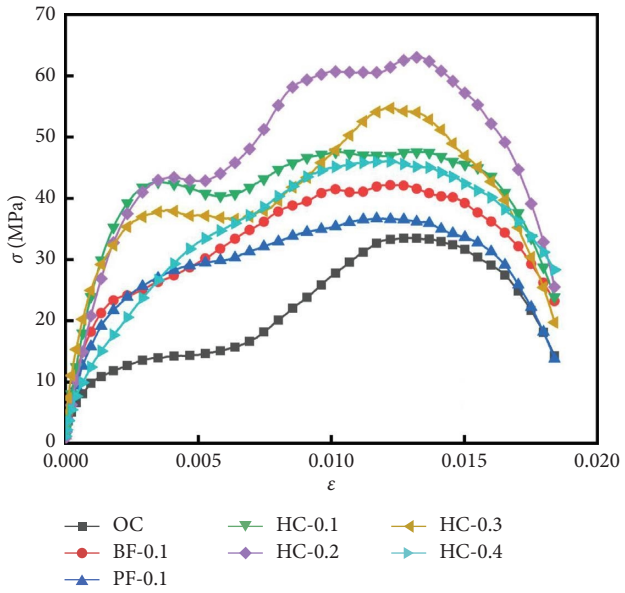

Figure 11: Stress-strain curve of the dynamic compression test.

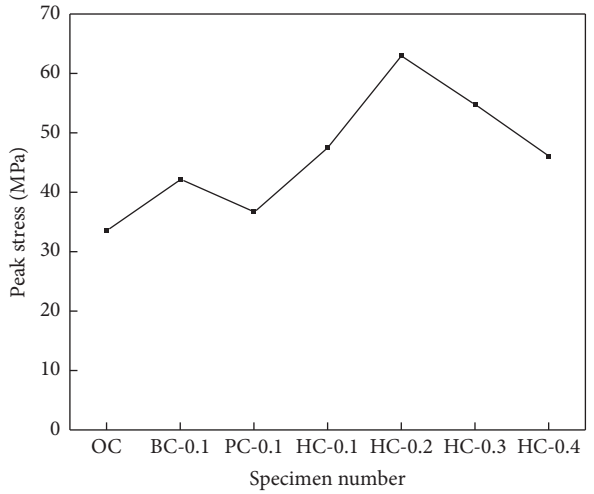

Figure 12: Peak stress.

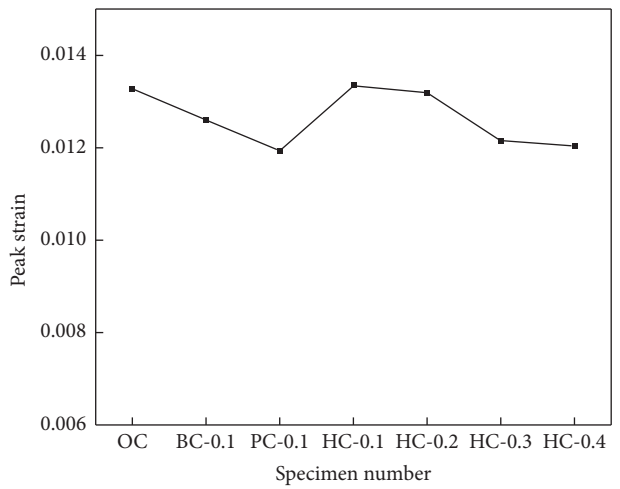

Figure 13: Peak strain.

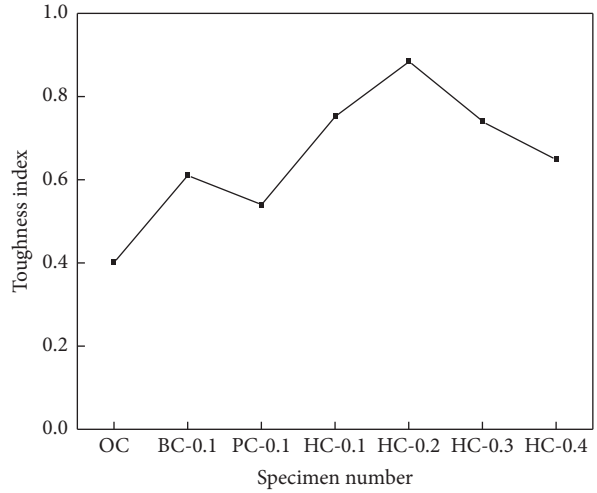

Figure 14: Resilience index.

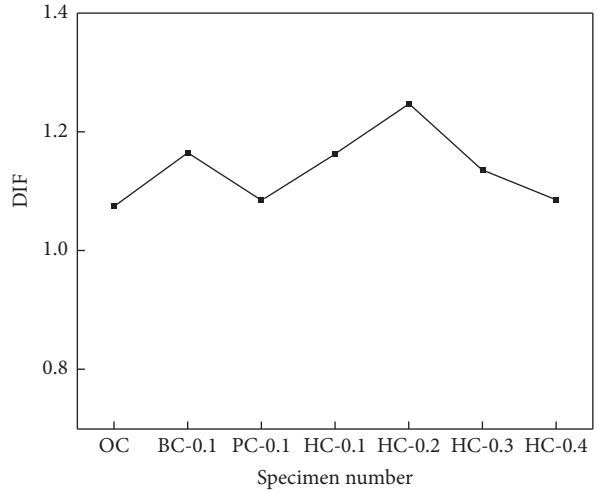

Figure 15: DIF.

compressive strength of each group, and the results are shown in Figure 15. It can be seen that with the growth of the fiber volume ratio, the dynamic strength and impact toughness index of LAC first increase and then decrease, which indicates that fibers, especially blended fibers, are beneficial to enhance the dynamic compressive strength of LAC and improve the toughness of LAC. The peak strain of the OC group was significantly different from the peak strain of LAC doped with fibers. The DIF results show that the fiber has an obvious polymer reinforcement effect on the LAC. The DIF value of the HC-0.2 group is the largest, and the strength enhancement effect is also the most obvious.

3.2.3. Energy Characteristic Analysis. The input energy of the specimen under the effect of dynamic compression is mainly converted into reflected energy, transmission energy, and absorption energy of the specimen. Under the stress balance state of the SHPB system, the energy absorbed by the specimen per unit volume is calculated as follows:

$$W_I = \frac{c_B A_B}{E_B} \int \sigma_I^2(t)\mathrm{d}t,$$
$$W_R = \frac{c_B A_B}{E_B} \int \sigma_R^2(t)\mathrm{d}t, \quad (8)$$
$$W_T = \frac{c_B A_B}{E_B} \int \sigma_T^2(t)\mathrm{d}t,$$

where W_I, W_R, and W_T are incident energy, reflected energy, and transmitted energy, respectively. c_B, A_B, and E_B are the wave velocity, cross-sectional area, and elastic modulus of the elastic rod, respectively. $\sigma_I(t)$, $\sigma_R(t)$, and $\sigma_T(t)$ are the incident stress, reflection stress, and transmission stress at time t, respectively.

Figure 16 shows the evolution law of incident energy, reflected energy, and transmission energy for each group of specimens under the effect load. On the whole, the incident energy, reflection energy, and transmission energy of the

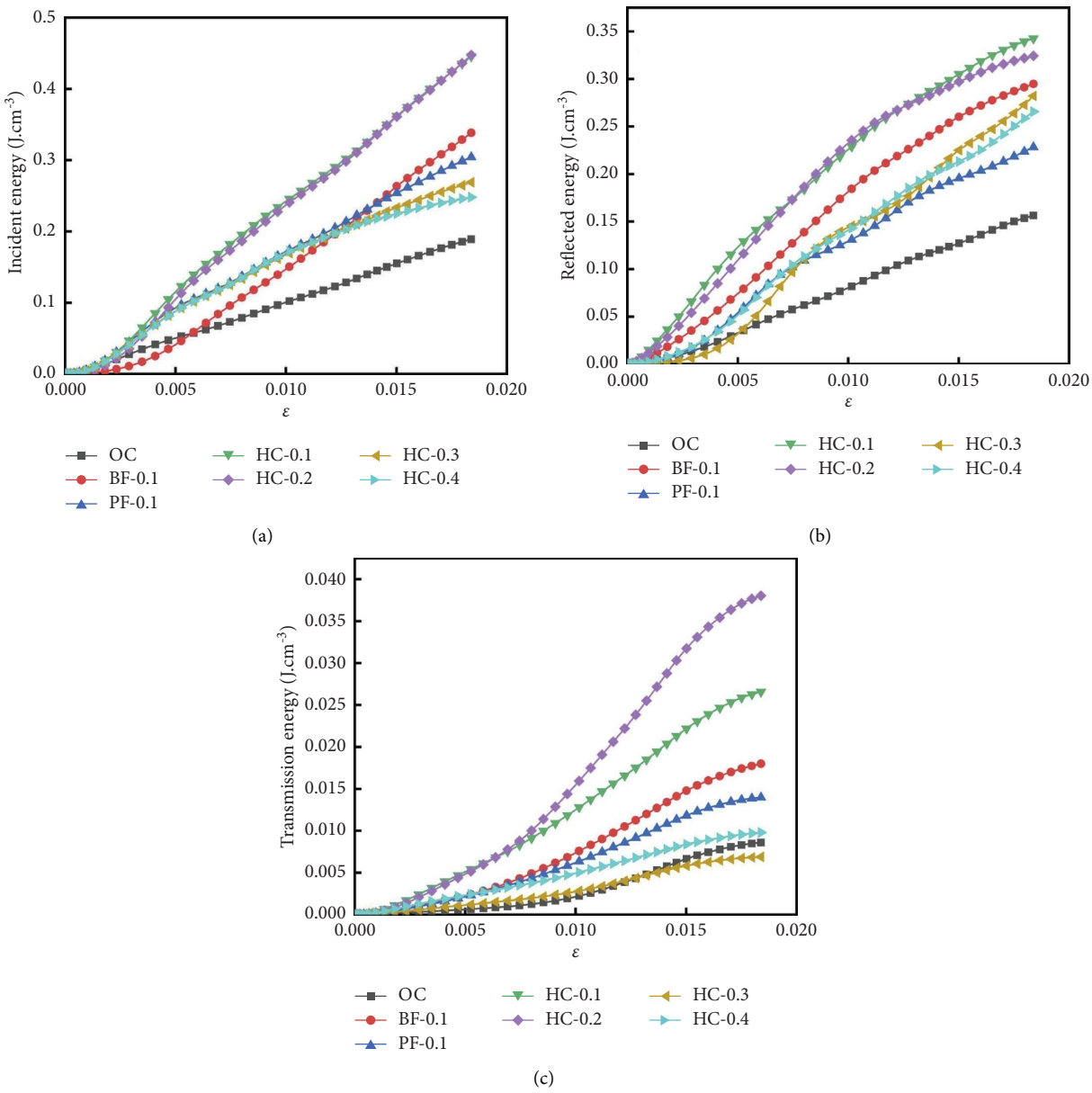

Figure 16: Energy evolution law. (a) Incident energy, (b) Reflected energy, (c) Transmission energy.

specimen grow first and then decline with the growth of the fiber volume ratio, which fully proves that adding fibers into the LAC is beneficial to improving the performance of the lightweight aggregate concrete. In terms of energy absorption capacity, the influence of blended fiber is better than that of single blended fiber, and the HC-0.2 group has the best performance.

4. Microstructure and EDS Analysis

4.1. SEM Microstructure. The failure morphology of the specimen is shown in Figure 17. It can be seen from Figures 17(a)–17(c) that LAC without fibers has large cracks inside and that HFLAC is relatively dense. This is mainly because the bridging effect of fibers enhances the compactness of the lightweight aggregate concrete, thereby improving the strength and toughness of the LAC. Due to the difference in physical and mechanical properties of basalt fiber and polypropylene fiber, the two can play an inhibitory role in different crack development stages of concrete, thereby changing the energy conversion mechanism of concrete and improving the ductility and toughness of concrete. Generally, fibers with a smaller size mainly inhibit the initiation and initial propagation of cracks, while fibers with a larger size mainly inhibit the expansion and penetration of macroscopic cracks. Due to the higher stiffness of basalt fiber, the bonding performance with the lightweight aggregate concrete matrix is better. Compared with polypropylene fiber, basalt fiber is more conducive to improving the strength of lightweight aggregate concrete; polypropylene fiber has less stiffness and ductility, which effectively reduces the crack penetration rate of lightweight aggregate

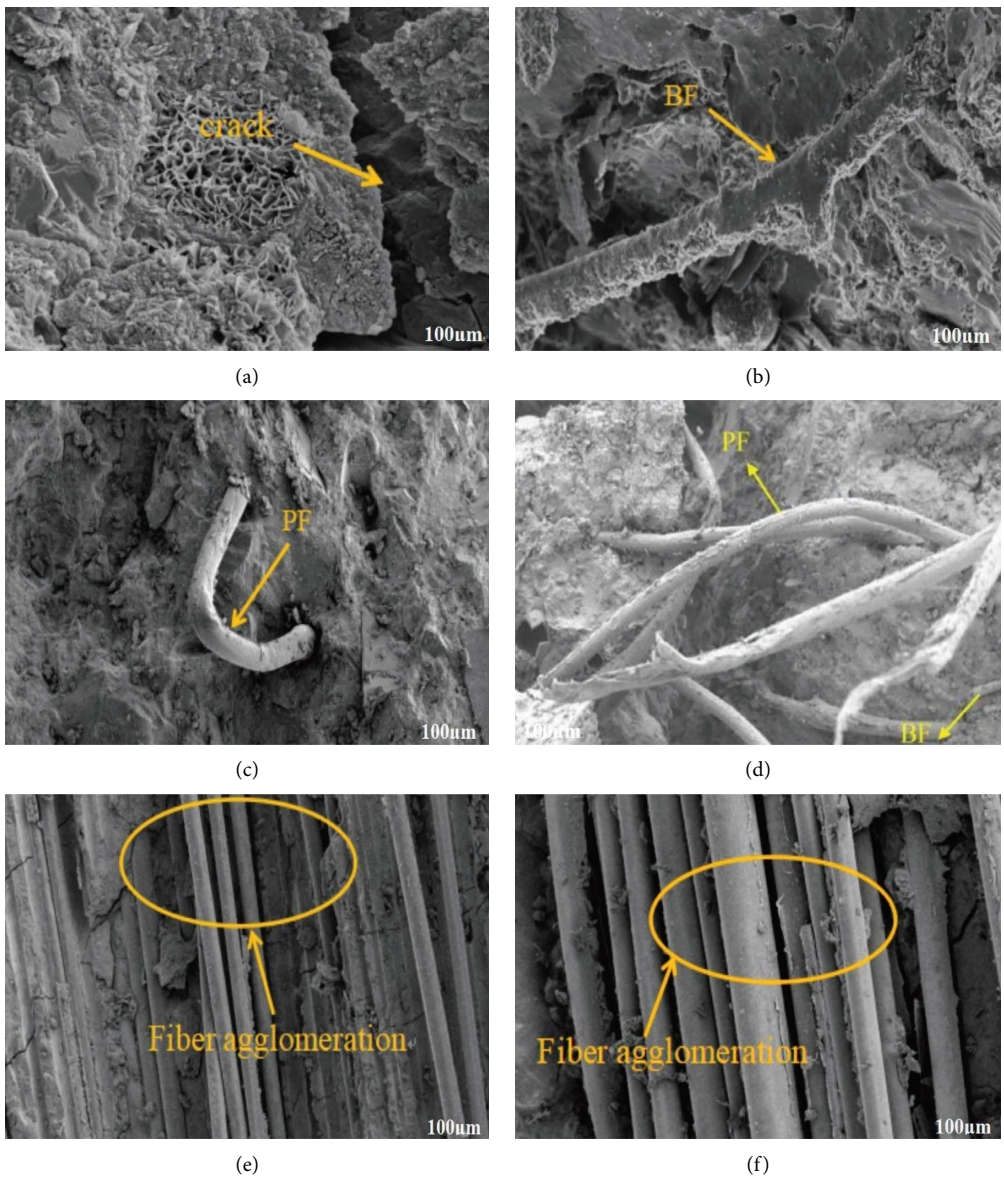

Figure 17: SEM microstructure. (a) OC group. (b) BF-0.1 group. (c) PF-0.1 group. (d) HC-0.2 group. (e) HC-0.3 group. (f) HC-0.4 group.

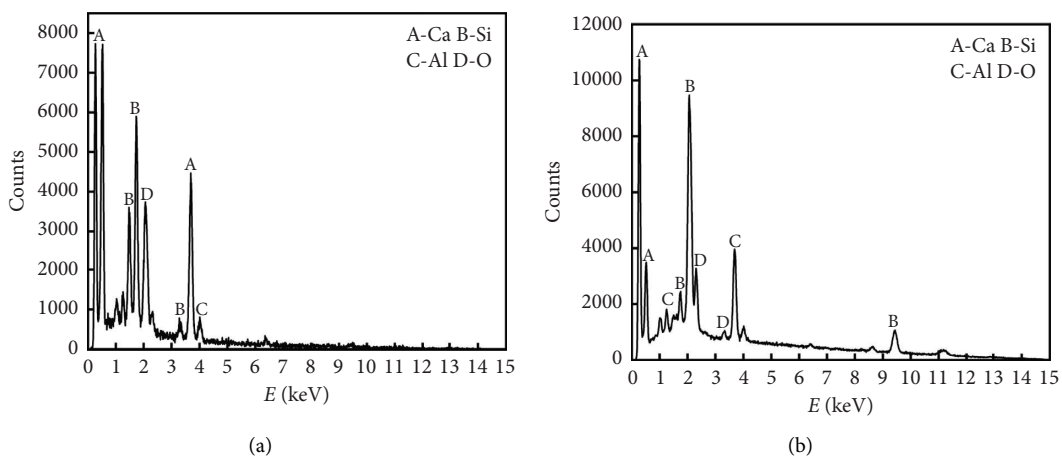

Figure 18: EDS test results. (a) OC group. (b) HC-0.2 group.

concrete, thus reducing the elastic strain energy release rate and dissipation energy conversion rate of lightweight aggregate concrete. It can be seen from Figures 17(d)–17(f) that when the volume content of the mixed basalt fiber and polypropylene fiber is too large, the dispersion uniformity of the basalt fiber and the polypropylene fiber is reduced, which affects the basalt fiber, polypropylene fiber and concrete matrix. The bonding properties between the basalt fibers and polypropylene fibers show a larger pull-out length. Therefore, the synergistic effect of basalt fiber and polypropylene fiber effectively inhibits the propagation and penetration of cracks in the lightweight aggregate concrete, but when the fiber volume ratio is too large, it is easy to form agglomeration in the lightweight aggregate concrete.

4.2. EDS Test. Based on the EDS test technology, the chemical element compositions of the OC group and the HC-0.2 group are given, as shown in Figure 18. It can be seen that compared with the ordinary lightweight aggregate concrete samples, the calcium and aluminum contents in the chemical composition formed in the fiber lightweight aggregate concrete are higher, which further promotes the absorption of Al and forms C-S-H gel, making the sample more dense and effectively enhances the strength and toughness of LAC.

5. Conclusions

(1) Basalt fiber and polypropylene fiber improve the strength of lightweight aggregate concrete, and the lifting effect of hybrid fiber is more obvious. Basalt fiber improves the strength of LAC more than polypropylene fiber, and the fiber volume ratio makes it easy to form fiber agglomeration, which reduces the strength of LAC. The incorporation of fibers into lightweight aggregate concrete significantly increases the elastic modulus, peak strain, and ultimate strain, which effectively enhances the toughness of LAC. This has a certain reference value for the application of fiber lightweight aggregate concrete in high-rise buildings or super high-rise buildings.

(2) Based on the Lemaitre equivalent strain assumption principle, the compressive damage constitutive model of HFLAC is deduced. According to the test data, the model parameters are determined, and the compressive damage constitutive equation of HFLAC is established. The test curves are compared and analyzed, and it is found that the two have a good degree of fit, which proves the accuracy of the proposed damage constitutive model.

(3) The dynamic compression performance test found that the fiber had a significant polymer reinforcement effect on lightweight aggregate concrete, which had a significant impact on the stress-strain relationship of lightweight aggregate concrete. It effectively enhanced the dynamic compression strength and toughness of LAC and improved the energy absorption capacity of LAC. Among them, the HC-0.2 group showed the best performance.

(4) Based on the microstructure and EDS test analysis, it is found that there are large cracks in the ordinary LAC and the HFLAC is denser due to the high content of calcium and aluminum. The basalt fiber has high stiffness and high adhesion with the lightweight aggregate concrete matrix, while the good ductility of polypropylene fiber is conducive to its inhibition of the expansion and coalescence of macrocracks. The synergistic effect of the two improves the strength and toughness of LAC.

Data Availability

The data used to support the findings of this study are included within the article.

Conflicts of Interest

The authors declare that there are no conflicts of interest.

Acknowledgments

The financial supports for the study were provided by Key Projects of Natural Science Research in Anhui Universities under Grant no. KJ2021A1234.

References

[1] U. I. Mohammad Momeen, *Feasibility Study of Ground palm Oil Fuel Ash as Partial Cement Replacement Material in Oil palm Shell Lightweight concrete/Mohammad Momeen Ul Islam*, Doctoral dissertation, University of Malaya), Malaya, 2015.

[2] M. M. U. Islam, J. Li, Y. F. Wu, R. Roychand, and M. Saberian, "Design and strength optimization method for the production of structural lightweight concrete: an experimental investigation for the complete replacement of conventional coarse aggregates by waste rubber particles," *Resources, Conservation and Recycling*, vol. 184, p. 106390, 2022.

[3] M. M. U. Islam, K. H. Mo, U. J. Alengaram, and M. Z. Jumaat, "Mechanical and fresh properties of sustainable oil palm shell lightweight concrete incorporating palm oil fuel ash," *Journal of Cleaner Production*, vol. 115, pp. 307–314, 2016.

[4] F. Ding, X. Wu, P. Xiang, and Y. Chen, "New damage ratio strength criterion for concrete and lightweight aggregate concrete[J]," *ACI Structural Journal*, vol. 118, no. 6, pp. 165–178, 2021.

[5] Z. H. Deng, H. Q. Huang, B. Ye, H. Wang, and P. Xiang, "Investigation on recycled aggregate concretes exposed to high temperature by biaxial compressive tests," *Construction and Building Materials*, vol. 244, Article ID 118048, 2020.

[6] J. Chen, W. Wang, F. X. Ding et al., "Behavior of an Advanced Bolted Shear Connector in Prefabricated Steel-concrete Composite Beams (Open Access)[J]," *Materials*, vol. 12, no. 18, 2958 pages, 2019.

[7] M. M. U. Islam, "Investigation of tensile creep for ultra-high-performance fiber reinforced concrete (UHPFRC) for the long-term," *Construction and Building Materials*, vol. 305, Article ID 124752, 2021.

[8] M. M. U. Islam, "Investigation of long-term tension stiffening mechanism for ultra-high-performance fiber reinforced concrete (UHPFRC)," *Construction and Building Materials*, vol. 321, Article ID 126310, 2022.

[9] M. M. U. Islam, *[EMBARGOED] Investigation of Tensile Creep and Tension Stiffening Behaviour for Ultra-high-performance Fiber Reinforced Concrete (UHPFRC)*, Doctoral dissertation), Beijing China, 2019.

[10] S. Kurugöl, L. Tanaçan, and H. Y. Ersoy, "Young's modulus of fiber-reinforced and polymer-modified lightweight concrete composites," *Construction and Building Materials*, vol. 22, no. 6, pp. 1019–1028, 2008.

[11] E. Güneyisi, M. Gesoğlu, and S. İpek, "Effect of steel fiber addition and aspect ratio on bond strength of cold-bonded fly ash lightweight aggregate concretes," *Construction and Building Materials*, vol. 47, pp. 358–365, 2013.

[12] T. Wu, Y. Sun, X. Liu, and H. Wei, "Flexural behavior of steel fiber–reinforced lightweight Aggregate concrete beams reinforced with glass fiber–reinforced polymer bars," *Journal of Composites for Construction*, vol. 23, no. 2, Article ID 04018081, 2019.

[13] M. Zhao, M. Zhao, M. Chen, J. Li, and D. Law, "An experimental study on strength and toughness of steel fiber reinforced expanded-shale lightweight concrete," *Construction and Building Materials*, vol. 183, pp. 493–501, 2018.

[14] H. T. Wang and L. C. Wang, "Experimental study on static and dynamic mechanical properties of steel fiber reinforced lightweight aggregate concrete," *Construction and Building Materials*, vol. 38, pp. 1146–1151, 2013.

[15] H. Wei, T. Wu, and X. Yang, "Properties of lightweight aggregate concrete reinforced with carbon and/or polypropylene fibers," *Materials*, vol. 13, no. 3, p. 640, 2020.

[16] J. M. Moreno-Maroto, A. L. Beaucour, B. González-Corrochano, and J. Alonso-Azcarate, "Study of the suitability of a new structural concrete manufactured with carbon fiber reinforced lightweight aggregates sintered from wastes," *Materiales de Construcción*, vol. 69, no. 336, p. e204, 2019.

[17] T. Wu, X. Yang, H. Wei, and X. Liu, "Mechanical properties and microstructure of lightweight aggregate concrete with and without fibers," *Construction and Building Materials*, vol. 199, pp. 526–539, 2019.

[18] J. M. Moreno-Maroto, B. González-Corrochano, J. Alonso-Azcárate, L. Rodriguez, and A. Acosta, "Manufacturing of lightweight aggregates with carbon fiber and mineral wastes," *Cement and Concrete Composites*, vol. 83, pp. 335–348, 2017.

[19] X. Liu, T. Wu, and Y. Liu, "Stress-strain relationship for plain and fibre-reinforced lightweight aggregate concrete," *Construction and Building Materials*, vol. 225, pp. 256–272, 2019.

[20] X. Liu, T. Wu, H. Chen, and Y. Liu, "Compressive stress-strain behavior of CFRP-confined lightweight aggregate concrete reinforced with hybrid fibers," *Composite Structures*, vol. 244, Article ID 112288, 2020.

[21] T. Wu, Y. Sun, X. Liu, and Y. Cao, "Comparative study of the flexural behavior of steel fiber-reinforced lightweight aggregate concrete beams reinforced and prestressed with CFRP tendons," *Engineering Structures*, vol. 233, Article ID 111901, 2021.

[22] F. G. Cunha, Z. L. M. Sampaio, and A. E. Martinelli, "Fiber-reinforced lightweight concrete formulated using multiple residues," *Construction and Building Materials*, vol. 308, Article ID 125035, 2021.

[23] M. Said, M. A. Adam, A. E. Arafa, and A. Moatasem, "Improvement of punching shear strength of reinforced lightweight concrete flat slab using different strengthening techniques," *Journal of Building Engineering*, vol. 32, Article ID 101749, 2020.

[24] G. Murali, S. R. Abid, M. Amran, R. Fediuk, N. Vatin, and M. Karelina, "Combined effect of multi-walled carbon nanotubes, steel fibre and glass fibre mesh on novel two-stage expanded clay aggregate concrete against impact loading," *Crystals*, vol. 11, no. 7, p. 720, 2021.

[25] X. Infant Alex and K. Arunachalam, "Flexural behavior of fiber reinforced lightweight concrete," *Revista de la construcción*, vol. 18, no. 3, pp. 536–544, 2019.

[26] K. Yoo-Jae and T. G. Harmon, "Analytical model for confined lightweight aggregate concrete[J]," *ACI Materials Journal*, vol. 103, no. 2, p. 263, 2006.

[27] C. X. Qian and P. Stroeven, "Development of hybrid polypropylene-steel fibre-reinforced concrete," *Cement and Concrete Research*, vol. 30, no. 1, pp. 63–69, 2000.

[28] A. M. López-Buendía, M. D. Romero-Sánchez, V. Climent, and C. Guillem, "Surface treated polypropylene (PP) fibres for reinforced concrete," *Cement and Concrete Research*, vol. 54, pp. 29–35, 2013.

[29] L. H. Xu, B. Huang, B. Li, and N. Xiao, "Study on the stress-strain relation of polypropylene fiber reinforced concrete under cyclic compression [J]," *China Journal of Civil Engineering*, vol. 52, no. 04, pp. 1–12, 2019.

[30] H. Mazaheripour, S. Ghanbarpour, S. H. Mirmoradi, and I. Hosseinpour, "The effect of polypropylene fibers on the properties of fresh and hardened lightweight self-compacting concrete," *Construction and Building Materials*, vol. 25, no. 1, pp. 351–358, 2011.

[31] G. W. Leong, K. H. Mo, Z. P. Loh, and Z. Ibrahim, "Mechanical properties and drying shrinkage of lightweight cementitious composite incorporating perlite microspheres and polypropylene fibers," *Construction and Building Materials*, vol. 246, Article ID 118410, 2020.

[32] H. Tanyildizi, "Statistical analysis for mechanical properties of polypropylene fiber reinforced lightweight concrete containing silica fume exposed to high temperature," *Materials & Design*, vol. 30, no. 8, pp. 3252–3258, 2009.

[33] S. P. Yap, C. H. Bu, U. J. Alengaram, K. H. Mo, and M. Z. Jumaat, "Flexural toughness characteristics of steel–polypropylene hybrid fibre-reinforced oil palm shell concrete," *Materials & Design*, vol. 57, pp. 652–659, 2014.

[34] S. B. Daneti, T. H. Wee, and T. S. Thangayah, "Effect of polypropylene fibres on the shrinkage cracking behaviour of lightweight concrete," *Magazine of Concrete Research*, vol. 63, no. 11, pp. 871–881, 2011.

[35] J. J. Li, J. G. Niu, C. J. Wan, B. Jin, and Y. l. Yin, "Investigation on mechanical properties and microstructure of high performance polypropylene fiber reinforced lightweight aggregate concrete," *Construction and Building Materials*, vol. 118, pp. 27–35, 2016.

[36] X. Sun, Z. Gao, P. Cao, and C. Zhou, "Mechanical properties tests and multiscale numerical simulations for basalt fiber reinforced concrete," *Construction and Building Materials*, vol. 202, pp. 58–72, 2019.

[37] R. Ralegaonkar, H. Gavali, P. Aswath, and S. Abolmaali, "Application of chopped basalt fibers in reinforced mortar: a review," *Construction and Building Materials*, vol. 164, pp. 589–602, 2018.

[38] V. J. John and B. Dharmar, "Influence of basalt fibers on the mechanical behavior of concrete—a review," *Structural Concrete*, vol. 22, no. 1, pp. 491–502, 2021.

[39] X. Wu, S. Wang, J. Yang, and F. Zhang, "Experimental study on mechanical performances of different fibre reinforced

lightweight concretes[J]," *Revista Romana de Materiale*, vol. 49, no. 3, pp. 434–442, 2019.

[40] Y. Zeng, P. Sun, A. Tang, and X. Zhou, "Shear performance of lightweight aggregate concrete with and without chopped fiber reinforced," *Construction and Building Materials*, vol. 263, Article ID 120187, 2020.

[41] L. R. Mailyan, A. N. Beskopylny, B. Meskhi, S. A. Stel'makh, E. M. Shcherban, and O. Ananova, "Optimization of composition and technological factors for the lightweight fiber-reinforced concrete production on a combined aggregate with an increased coefficient of structural quality," *Applied Sciences*, vol. 11, no. 16, p. 7284, 2021.

[42] Y. Chi, L. Xu, and Y. Zhang, "Experimental study on hybrid fiber–reinforced concrete subjected to uniaxial compression," *Journal of Materials in Civil Engineering*, vol. 26, no. 2, pp. 211–218, 2014.

[43] K. F. Li, C. Q. Yang, W. Huang et al., "Effects of hybrid fibers on workability, mechanical, and time-dependent properties of high strength fiber-reinforced self-consolidating concrete," *Construction and Building Materials*, vol. 277, Article ID 122325, 2021.

[44] Y. Xia and G. Xian, "Hybrid basalt/flax fibers reinforced polymer composites and their use in confinement of concrete cylinders," *Advances in Structural Engineering*, vol. 23, no. 5, pp. 941–953, 2020.

[45] Z. Deng, B. Liu, B. Ye, and P. Xiang, "Mechanical behavior and constitutive relationship of the three types of recycled coarse aggregate concrete based on standard classification," *Journal of Material Cycles and Waste Management*, vol. 22, no. 1, pp. 30–45, 2020.

[46] B. Chen, C. Gu, T. Bao, B. Wu, and H. Su, "Failure analysis method of concrete arch dam based on elastic strain energy criterion," *Engineering Failure Analysis*, vol. 60, pp. 363–373, 2016.

[47] V. Dattoma and S. Giancane, "Evaluation of energy of fatigue damage into GFRC through digital image correlation and thermography," *Composites Part B: Engineering*, vol. 47, pp. 283–289, 2013.

[48] L. Kachanov, *Introduction to Continuum Damage mechanics [M]*, Springer Science & Business Media, Heidelberg, Germany, 1986.